Veterinary Integrative Sciences 2024; 22(2): 419 - 444 DOI; 10.12982/VIS.2024.030

Vet Integr Sci

Veterinary Integrative Sciences

Faculty of Veterinary Medicine
Chiang Mai University

ISSN; 2629-9968 (online)

Website; www.vet.cmu.ac.th/cmvj

Research article

Unravelling key genes associated with ovine Brucellosis by differential gene expression analysis: A holistic bioinformatics study

Varsha Ramesh[1], Uma Bharathi Indrabalan[1], Swati Rani[1], Kuralayanapalya Puttahonnappa Suresh [1,*], Nagendra Nath Barman[2] and Azhahianambi Palavesam[3]

[1]ICAR-National Institute of Veterinary Epidemiology and Disease Informatics (NIVEDI), Yelahanka, Bengaluru-560064, India
[2]Assam Agricultural University, Khanapara, Guwahati, Assam-781022, India
[3]Tamil Nadu Veterinary and Animal Sciences University, Chennai, Tamil Nadu-600051, India

Abstract

Ovine Brucellosis, caused by *Brucella ovis* bacteria, is a pathognomonic reproductive infectious disease of sheep that causes epididymitis in rams (male sheep) and placental inflammation in ewes (female sheep) leading to reduced fertility. The specific molecular process that causes alterations in genome of sheep during brucellosis is not yet fully understood. This study aimed to identify key host genes associated with the pathogenesis of ovine brucellosis caused by *B. ovis*. The GSE35614 dataset containing six healthy and six *Brucella ovis* infected sample of rams in the chronic phase 2 was obtained from the NCBI GEO database to examine and detect any differences in gene expression (DEGs). Functional and pathway enrichment analyses of the DEGs were performed along with the construction of protein-protein interaction network. Next, functional modules and hub genes were clustered and identified respectively, using the MCODE plugin. As a result, a total of 316 differentially expressed genes were filtered according to the provided cut-off criteria. The enriched DEGs were related to extracellular matrix interaction, cell adhesion mediated by integrin, angiogenesis, and inflammatory response. Furthermore, the hub gene analysis resulted in five hub genes namely, FN1, FBN1, CDH1, CD44, and SPP1, were up-regulated during the infection which could lead to reproductive disorders in sheep. In conclusion, the DEGs, functional and pathways terms, along with hub genes identified in the current study can provide prospective targets for the early diagnosis and treatment of brucellosis and provide insight into the molecular mechanism underlying the alterations that occur during brucellosis in sheep.

Keywords: *Brucella ovis* infection, Differential gene expression, Epididymitis, Functional enrichment, Hub gene, PPI

***Corresponding author:** Kuralayanapalya Puttahonnappa Suresh, Principal Scientist-Biostatistics, Spatial Epidemiology lab, ICAR-National Institute of Veterinary Epidemiology and Disease Informatics (NIVEDI), Yelahanka, Bengaluru-560064, India. E-mail: suresh.kp@icar.gov.in.

Article history; *received manuscript: 3 August 2023,*
revised manuscript: 19 September 2023,
accepted manuscript: 17 October 2023,
published online: 25 October 2023
Academic editor: *Prapas Patchanee*

INTRODUCTION

Brucellosis is a highly contagious zoonotic disease caused by various species of the genus Brucella. Over half a million cases of the disease were reported annually worldwide (Pappas et al., 2006; Seleem et al., 2010). Brucellae are intracellular bacteria that cause brucellosis, a chronic disease of domestic and wild animals and humans. For these bacteria to cause disease, their capacity to penetrate, last for extended periods of time, and reproduce inside the host cell is essential. Sheep is one among the economically important domestic animal which is affected by brucellosis. The efficient income generation from sheep husbandry depends on growth rate and ewe reproduction performance i.e. conception rate and litter size. Therefore, these are important traits in sheep enterprise (Bashir et al., 2020), which is affected by brucellosis.

Brucella ovis (B.ovis), one of the Brucella species, causing brucellosis in sheep does not infect humans (Poester et al., 2013). *B.ovis* is a non-sporeforming, non-encapsulated, 0.7 to 1.2 m broad Gram-negative bacilli or coccobacilli (Blasco, 1990). Unlike the majority of Brucellae, *B.ovis* does not have urease activity and cannot convert nitrate to nitrite. It is characterized by testicular changes, reduced fertility due to poor semen quality in rams (male sheep) and sporadic miscarriages in ewes (female sheep) (Blasco, 1990; Carrera-Chávez et al., 2016). The chronic phase of the disease in rams is characterized by testicular atrophy and varying degrees of epididymis tail expansion. The testes often appear normal at the macroscopic level, but the formation of granulomas and calcification may be visible on the cut surface (Watt, 1970). Although it is not very virulent for nongravid uteri, *B.ovis* causes placentitis and abortion in pregnant ewes (Menzies, 2012).

B.ovis, the responsible bacterium, was initially discovered in 1952 in New Zealand (McFarlane et al., 1952) and it took 18 years to acknowledge *B.ovis* as a member of the genus (Meltzer et al., 2010). The disease has also been documented in Australia, the United States, Argentina, the former Soviet Union, Czechoslovakia, Romania, Hungary, France, Germany, Spain, Canada, Mexico, Uruguay, Peru, Chile, Brazil, and South Africa. In addition, it is also likely to exist in other nations that raise sheep. (Blasco, 1990). Despite the fact that India is considered a geographical hotspot for brucellosis, only one seroprevalence of *B.ovis* infection in sheep, has yet been reported (Shome et al., 2018).

Numerous studies have revealed that gene expression may play a role in the progression of the brucellosis disease in sheep. An infection with a smooth (S) virulent strain of brucellae has the power to change the host cell's gene expression, affecting immune responses that promote intracellular survival and the establishment of chronic infections (Rajashekara et al., 2006). However, *B.ovis* is a naturally rough (R) strain of Brucella species which lacks O-Polysaccharides on its LPS wall. Variations in gene expression pattern in sheep infected with Rough brucella, *B.ovis* has not been explored (Galindo et al., 2009). The crucial genes expressed during ovine brucellosis have, however, received relatively little attention. Moreover the hub genes, signaling pathways, and differentially expressed genes (DEGs) that may be linked to the host response to brucellosis have not yet been studied. Thus bioinformatic microarray gene expression and its functional pathway enrichment analysis can

be a useful method to identify the key genes responsible for the pathobiology of this disease.

The dataset GSE35614 is a gene expression data set based on microarray analysis which includes 12 samples of rams experimentally infected with a highly virulent strain of *Brucella ovis* (chronic phase 2). The dataset was processed using Limma package to identify 316 DEGs in the chronic phase 2 of infection compared to the control samples. By analyzing biological processes, creating protein-protein interaction (PPI) network enriched pathways, and identifying hub genes for brucellosis, it was possible to understand the molecular mechanism behind the rams' response to brucellosis.

MATERIALS AND METHODS

Gene expression dataset collection

Gene Expression Omnibus (GEO) database of NCBI (https://www.ncbi.nlm.nih.gov/geo/) was used to search for dataset (Table 1) on microarray gene expression (GSE35614) regarding Brucellosis of platform animal host *Bos taurus* and its sample animal host being *Ovis Aries. Brucella ovis* infected sheep samples from 12 rough virulent strains, 6 patients in chronic 2 phase, and 6 controls were included in the dataset. By using the GPL2112 Affymetrix Bovine genome array platform, the microarray analysis of gene expression in rams infected with a highly virulent strain of *Brucella ovis* was experimentally acquired (Karimizadeh et al., 2019).

Table 1 Information of GSE35615 microarray dataset retrieved from GEO database of NCBI.

Data	GSE35614
Platform	GPL2112
Experiment type	Expression profiling by array
Disease	Brucellosis
Object of study	*Ovis Aries*
Microarray providing mechanism	UNESP [Sao Paulo State University]
Address	FMVZ, Distrito de Rubião Júnior, Botucatu, São Paulo, Brazil
Number of samples (use/total)	12/12

Datasets preprocessing

The data was preprocessed using R statistical programming language. The series matrix files and appropriate annotations for the dataset were obtained from the GEO database. Groups of selected datasets were created based on the control and diseased stages. Then, preparation procedures were carried out in group sample (Karimizadeh et al., 2019). The dataset were normalized by the robust multichip averaging (RMA) method using affy packages of R (4.2.1) (Gupta et al., 2017).

Functional and pathway enrichment analysis

The Gene Ontology (GO) and Kyoto Encyclopedia of Genes and Genomes (KEGG) pathway were analyzed using the Database for Annotation, Visualization and Integrated Discovery (DAVID) online tool (https://david.ncifcrf.gov/) and was used at the functional level. The GO terms and KEGG terms were regarded as enriched with thresholds of P.value <0.05, which were set as the cut-off criterion. If a biological pathway or GO word had an adjusted P.value of 0.05 or lower, it was significantly overrepresented in the gene list (Zhu et al., 2019).

PPI network construction and module analysis

The PPI network of the DEGs was analyzed by the STRING database (https://string-db.org). An interaction confidence score > 0.4 was set as significant. The confidence score of the interaction is the probability value calculated based on both experimental and computational evidence such as text mining, high-throughput experiments, co-expression and gene fusion data, and information from other databases. The PPI network was visualized by Cytoscape software (version 3.9.1; The Cytoscape Consortium, New York City, NY, USA). The modules of the PPI network were analyzed by the Molecular Complex Detection (MCODE) plugin (Hogue and Groll, 2001). MCODE plugin detects densely connected modules in the PPI networks that might represent molecular complexes. Significant modules were screened out using the following default plugin cut-off criteria: degree cut-off:2, node score cut-off: 0.2, k-core: 2, and max depth: 100. The resulting nodes in the key modules are presented as highly connected proteins that may have important biological functions (Fang et al., 2020).

Identification of hub genes

The PPI network, which was constructed using the STRING database, downloaded as a simple interaction format (.tsv file), was visualized with Cytoscape, and examined with the CytoHubba plugin to determine the hub genes. Based on the three network metrics (degree, closeness, and betweenness), top ten genes were independently derived from the PPI network, and then common genes among these were chosen as hub genes. High degree centrality genes are frequently referred to as "hubs" in the network since they have numerous interactions with other genes. Betweenness quantifies how frequently a gene serves as a link or middleman between other genes in the network. High closeness centrality genes are ones that have numerous close connections to other genes and have an easy time passing information to and receiving it from other genes (Liu et al., 2019).

RESULTS

Microarray data processing

Raw data were normalized to fix the measured intensities among control and infected samples of the chronic2 phases of Ovis Aries infected with *Brucella ovis*. The differentially expressed DEGs were also screened out during this process. Figure 1 shows the distribution of data pre- and post-normalization, depicted by box plot and histogram.

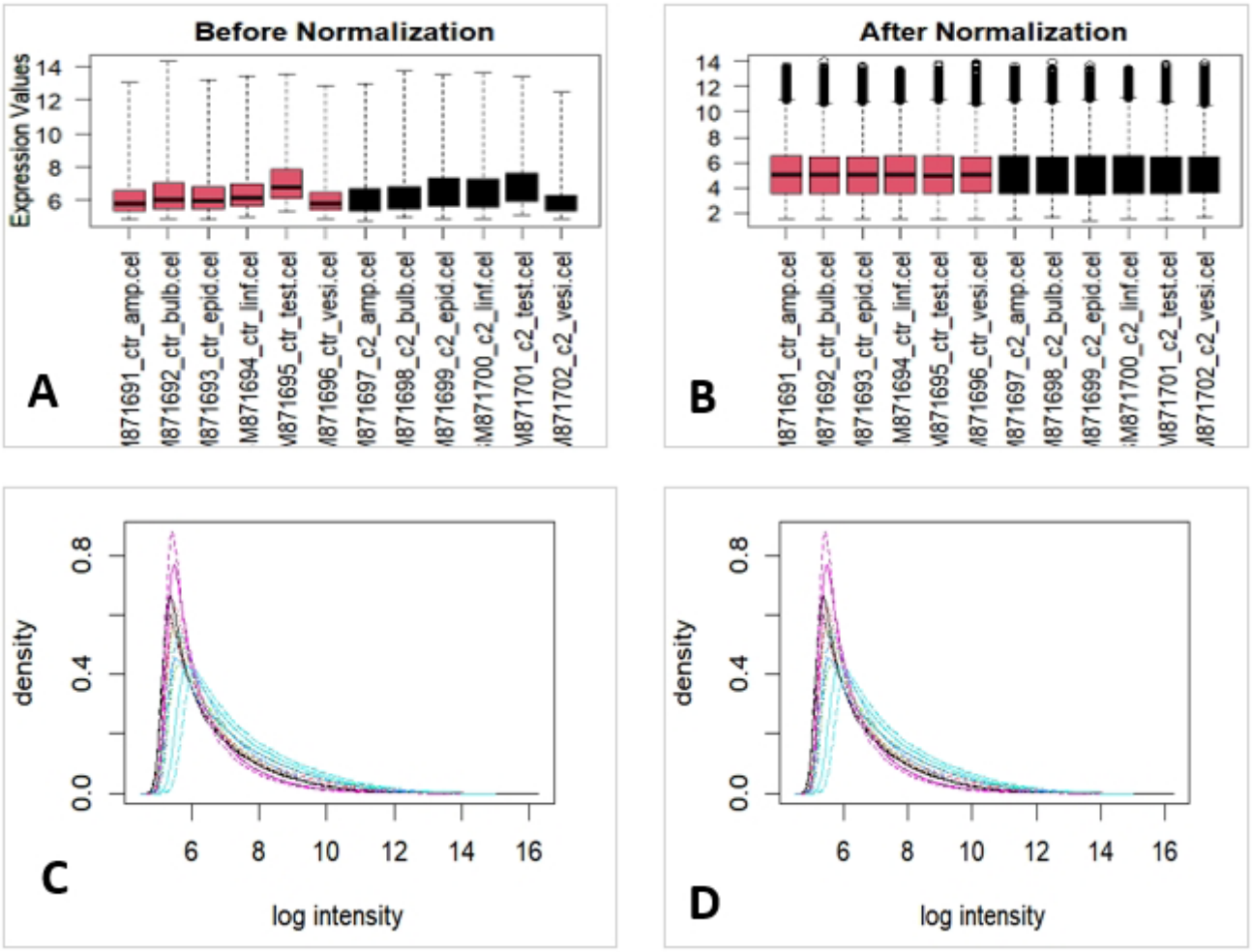

Figure 1 Normalization of microarray data from GEO (Accession No. GSE35614). Box plots of the raw microarray data pre-(A) and post normalization (B); the black color of the box represents data from uninfected(control) samples whereas red boxes represent the infected samples of chronic2 phase. The plot consists of boxes with a central line and two tails; the central line represents the median of the data, whereas, the tails represent the upper and lower quartile. Histogram of the raw data (C) pre-normalization and (D) post-normalization.

Identification of DEGs

A total of 316 DEGs from the sample of microarray data in rams experimentally infected with a rough virulent strain of *Brucella ovis* were shortlisted by comparing with controls and infected, and meeting the cut-off criterion logFC > 0.5 and adjusted p-value < 0.05. Among 316 DEGs, 75 genes were found to be downregulated, whereas 241 were found to be upregulated (Table 2). The top 50 genes of each up-regulated (Figure 2A) and downregulated (Figure 2B) DEGs from the sample dataset were clustered and represented as a heatmap.

Table 2 A total of 316 differentially expressed genes (DEGs) of GSE35614 identified by R statistical analysis. Cutoff criteria given as logFC < 0.5 and P.Value <0.05

Sl.No.	Symbols.ch2	BH.corrected.pvalue	fold.change.mean
		Down-regulated DEGs	
1	PRM1	7.55E-13	-1.92535
2	TNP2	0.001609	-1.05757
3	BVES	1.06E-10	-1.00314
4	SOSTDC1	1.81E-11	-0.93158
5	TKTL1	3.91E-12	-0.91479
6	LOC100848405	5.43E-12	-0.90023
7	RYR3	7.35E-11	-0.88009
8	TNP1	2.61E-10	-0.87951
9	HACD1	5.90E-14	-0.7797
10	MAL	4.83E-10	-0.77606
11	NUPR2	1.00E-10	-0.76163
12	ENTPD3	5.11E-14	-0.75942
13	IRS4	2.08E-13	-0.75865
14	INSL3	5.98E-15	-0.75774
15	CHCHD10	6.97E-14	-0.73895
16	SMARCD3	2.73E-10	-0.73243
17	COX6B2	1.67E-10	-0.72967
18	P4HTM	6.24E-09	-0.7125
19	PRKCB	2.12E-14	-0.7038
20	SLC46A2	1.32E-11	-0.70296
21	LOC508646	3.20E-13	-0.69666
22	PRM2	2.14E-10	-0.68841
23	GK	1.86E-13	-0.68728
24	FAM81A	6.08E-14	-0.6742
25	CUX2	2.97E-12	-0.67412
26	TRIM37	3.71E-12	-0.66724
27	DTX4	5.65E-13	-0.66669
28	SLITRK6	2.16E-10	-0.66156
29	FCAR	4.50E-08	-0.65921
30	ARHGEF25	2.43E-10	-0.65755
31	PARD6B	1.05E-08	-0.65191
32	MMP9	9.79E-10	-0.65154
33	CMC2	1.15E-10	-0.6464
34	CHGA	8.85E-15	-0.6438
35	VIP	2.82E-15	-0.62406
36	RPGRIP1	1.03E-12	-0.62181
37	BMP7	1.12E-13	-0.61305
38	CABYR	1.07E-13	-0.60853
39	RUFY3	1.28E-12	-0.59995
40	PNMT	7.45E-10	-0.59699
41	CFAP70	7.11E-12	-0.58922
42	LOC530077	1.13E-12	-0.57737
43	DLGAP4	2.07E-13	-0.57574

Table 2 A total of 316 differentially expressed genes (DEGs) of GSE35614 identified by R statistical analysis. Cutoff criteria given as logFC < 0.5 and P.Value <0.05 (Cont.)

Sl.No.	Symbols.ch2	BH.corrected.pvalue	fold.change.mean
Down-regulated DEGs			
44	ASB2	2.40E-12	-0.57236
45	PLIN5	1.10E-13	-0.56949
46	TCAIM	1.27E-13	-0.56769
47	FRMPD1	7.30E-12	-0.56337
48	ALDOB	1.77E-09	-0.56262
49	HCCS	1.30E-11	-0.55946
50	AQP7	0.001124	-0.55718
51	ITGB1BP2	7.66E-12	-0.55446
52	APOH	1.60E-09	-0.55132
53	UGGT2	2.37E-12	-0.54939
54	HOXA9	1.74E-11	-0.54928
55	ALS2CL	3.46E-12	-0.5482
56	INPP5A	3.42E-15	-0.53545
57	DES	6.68E-09	-0.5291
58	DNAJB1	9.94E-14	-0.52824
59	CDCA7L	2.13E-14	-0.52809
60	CELA2A	2.11E-10	-0.52682
61	PDZRN4	1.09E-10	-0.52653
62	FLNA	1.40E-05	-0.52517
63	POLR1E	2.31E-15	-0.52444
64	KLHDC8B	1.78E-10	-0.52048
65	NDRG4	6.50E-11	-0.51316
66	ANGPT1	1.19E-14	-0.51129
67	RBM38	2.42E-12	-0.51077
68	SCML1	1.82E-11	-0.50965
69	DKKL1	6.68E-11	-0.50894
70	BCORL1	9.71E-12	-0.5077
71	RET	5.71E-07	-0.50618
72	SYCP3	8.09E-14	-0.5061
73	CHD6	6.54E-14	-0.50273
74	KANSL1	1.38E-11	-0.50059
75	DHX35	7.45E-15	-0.50002
Up-regulated DEGs			
76	FLI1	2.85E-13	0.500939
77	EDEM3	2.58E-14	0.501458
78	HBB	2.48E-08	0.501925
79	HOXB7	2.74E-12	0.502351
80	RABGAP1L	5.50E-14	0.502563
81	CKAP4	2.06E-10	0.503042
82	TNXB	2.64E-09	0.503172
83	MYF6	2.01E-12	0.504988
84	HTRA1	4.31E-14	0.506009
85	PPP1R1B	9.73E-10	0.506113

Table 2 A total of 316 differentially expressed genes (DEGs) of GSE35614 identified by R statistical analysis. Cutoff criteria given as logFC < 0.5 and P.Value <0.05 (Cont.)

Sl.No.	Symbols.ch2	BH.corrected.pvalue	fold.change.mean
Down-regulated DEGs			
86	NRROS	1.12E-11	0.507276
87	CDH13	1.19E-08	0.507598
88	BSP3	2.17E-12	0.509253
89	GOLM1	3.27E-09	0.509828
90	SACM1L	1.51E-14	0.509896
91	SFRP4	3.05E-10	0.51006
92	IDH1	1.35E-14	0.510918
93	CDH1	2.90E-15	0.511708
94	NFIB	1.11E-12	0.512688
95	B2M	2.16E-09	0.512949
96	SHISA3	2.54E-15	0.51325
97	PPL	2.67E-10	0.513709
98	LOC789258	2.25E-15	0.515142
99	DHRS4	2.82E-15	0.516064
100	ANKH	1.09E-11	0.517196
101	IFI16	1.27E-12	0.518019
102	CCNL1	1.42E-13	0.518389
103	CD34	8.15E-10	0.519074
104	PMAIP1	4.32E-13	0.519627
105	KDM1B	5.76E-15	0.519818
106	TP53INP2	6.59E-13	0.519925
107	ECSCR	2.44E-07	0.520572
108	DNAJC3	8.30E-13	0.521731
109	SULT1C4	9.90E-15	0.522316
110	SCIN	4.42E-10	0.522506
111	LIPA	2.12E-10	0.522755
112	LEPROT	1.87E-07	0.522939
113	NID1	1.10E-07	0.523592
114	PTGDS	5.41E-14	0.523696
115	REXO2	1.15E-13	0.52404
116	CPE	2.21E-14	0.524284
117	HAS2	9.73E-15	0.52441
118	AOC1	2.41E-10	0.524661
119	STEAP3	1.30E-14	0.527015
120	BACE2	2.77E-08	0.527222
121	TRIM2	1.79E-14	0.52738
122	FRMD8	3.27E-09	0.528456
123	MCC	2.18E-11	0.529257
124	LOC782922	2.09E-12	0.529489
125	RAB32	1.21E-08	0.531737
126	EIF2AK3	1.42E-15	0.532706
127	MAGEF1	6.31E-09	0.533021
128	CLCA2	3.84E-14	0.53416

Table 2 A total of 316 differentially expressed genes (DEGs) of GSE35614 identified by R statistical analysis. Cutoff criteria given as logFC < 0.5 and P.Value <0.05 (Cont.)

Sl.No.	Symbols.ch2	BH.corrected.pvalue	fold.change.mean
Down-regulated DEGs			
129	BOLA-NC1	1.89E-12	0.53448
130	LDB2	3.64E-15	0.536543
131	ARL5B	1.04E-13	0.539837
132	NNAT	1.78E-09	0.539924
133	CASP4	4.02E-14	0.541848
134	MAOB	1.58E-12	0.542759
135	CRYM	7.89E-11	0.545281
136	CFI	1.44E-14	0.546378
137	ELOVL7	4.45E-13	0.547407
138	PRSS23	5.46E-13	0.54825
139	SKIC3	8.41E-13	0.551485
140	KERA	2.60E-09	0.551568
141	ITGBL1	2.74E-12	0.551927
142	ARHGAP26	5.51E-11	0.553986
143	CD44	3.09E-09	0.554675
144	ACOX1	3.35E-12	0.557574
145	CLIC5	2.99E-13	0.557887
146	PROCR	2.13E-09	0.558018
147	MAGEL2	2.18E-11	0.55824
148	CLDN2	4.34E-11	0.558668
149	TMEM163	7.66E-13	0.559258
150	SLC9A3R1	1.34E-07	0.559384
151	NDFIP2	3.87E-09	0.559713
152	CLDN11	1.16E-09	0.560438
153	NCL	4.13E-08	0.560772
154	ALCAM	2.71E-12	0.5611
155	UACA	9.14E-15	0.561334
156	SPON1	3.08E-08	0.56151
157	NEB	2.21E-14	0.56301
158	FKBP14	4.61E-11	0.564515
159	DPP4	1.65E-07	0.565179
160	ZNF175	2.50E-11	0.565815
161	MBP	7.91E-15	0.56641
162	STC1	1.43E-15	0.568061
163	EPB41L2	2.32E-12	0.568224
164	TGM2	2.66E-09	0.569598
165	LOC511229	8.58E-13	0.571509
166	TMEM45A	1.03E-12	0.572951
167	PON2	2.49E-12	0.573744
168	LPAR6	2.60E-12	0.574302
169	FAM221A	1.10E-13	0.574464
170	CLTRN	1.13E-12	0.575351
171	CPT1A	3.31E-06	0.579486

Table 2 A total of 316 differentially expressed genes (DEGs) of GSE35614 identified by R statistical analysis. Cutoff criteria given as logFC < 0.5 and P.Value <0.05 (Cont.)

Sl.No.	Symbols.ch2	BH.corrected.pvalue	fold.change.mean
		Down-regulated DEGs	
172	FAM43A	1.79E-11	0.579516
173	ANXA2	6.14E-10	0.580652
174	GATM	2.20E-12	0.580661
175	ADK	1.05E-13	0.582516
176	C15H11orf52	2.79E-13	0.583014
177	MYH7	1.24E-08	0.585743
178	C16H1orf21	8.38E-10	0.587714
179	PALMD	1.45E-15	0.589745
180	PIP4K2A	2.29E-13	0.591585
181	FCGRT	1.45E-15	0.59175
182	RWDD3	1.47E-12	0.592468
183	PDLIM1	1.63E-14	0.595071
184	AGR2	7.87E-11	0.595904
185	GPHN	2.44E-14	0.597722
186	ATP13A4	6.42E-12	0.598275
187	SLC44A4	3.50E-12	0.600028
188	DPYS	1.75E-13	0.600407
189	RHPN2	6.77E-15	0.601644
190	LGALS3	2.22E-14	0.602735
191	SNAI2	8.11E-10	0.605473
192	COL21A1	1.17E-12	0.607427
193	CKM	3.24E-10	0.608114
194	GM2A	2.87E-14	0.608347
195	ATF6	4.73E-10	0.608558
196	MUC19	2.18E-14	0.612164
197	XYLB	1.43E-15	0.612623
198	AKR1C4	2.08E-12	0.613931
199	CGNL1	1.54E-14	0.614053
200	MYH3	6.30E-15	0.615902
201	CD36	2.61E-09	0.616242
202	FSTL1	4.10E-08	0.616936
203	SPARC	1.53E-08	0.617578
204	ISLR	2.65E-13	0.618371
205	S100A10	1.55E-09	0.620474
206	MAP3K7CL	3.64E-15	0.623747
207	CLEC3B	1.70E-14	0.625342
208	LDLRAD3	4.65E-15	0.625848
209	LUM	3.82E-12	0.626142
210	MYH1	6.31E-15	0.626604
211	ARHGAP29	7.85E-15	0.629042
212	TFPI2	4.91E-13	0.629777
213	TM9SF1	2.28E-10	0.640041
214	LTBP2	4.86E-13	0.643481

Table 2 A total of 316 differentially expressed genes (DEGs) of GSE35614 identified by R statistical analysis. Cutoff criteria given as logFC < 0.5 and P.Value <0.05 (Cont.)

Sl.No.	Symbols.ch2	BH.corrected.pvalue	fold.change.mean
Down-regulated DEGs			
215	BOLA-DQB	7.54E-13	0.644594
216	TNNT3	2.83E-15	0.644658
217	ANKRD1	3.61E-14	0.645698
218	TNFAIP6	1.32E-05	0.648071
219	PTX3	1.50E-15	0.648583
220	RAMP1	2.25E-12	0.652044
221	LRRC17	1.28E-09	0.652129
222	MYLIP	1.67E-08	0.652269
223	TGFB3	8.09E-15	0.652501
224	LGMN	6.53E-07	0.653751
225	EMP1	3.50E-14	0.657124
226	FHDC1	5.26E-08	0.661629
227	TMEM30B	1.28E-12	0.669839
228	TENT5A	3.09E-13	0.670304
229	METTL9	2.26E-15	0.670727
230	STRIP2	1.29E-14	0.672455
231	TEK	6.62E-10	0.674383
232	HSD17B6	5.20E-14	0.677038
233	PERP	1.90E-05	0.680044
234	TSPAN12	7.99E-11	0.686985
235	MT2A	5.92E-12	0.687141
236	FNDC3B	2.91E-11	0.692211
237	TRMT10B	4.89E-12	0.692628
238	COL5A2	0.000595	0.694388
239	EMCN	1.49E-09	0.694785
240	S100G	4.09E-10	0.697376
241	LRP11	1.07E-13	0.703257
242	MDFIC	3.24E-13	0.706552
243	MGP	3.16E-10	0.707024
244	CD47	3.39E-14	0.713833
245	PODXL	2.54E-13	0.715878
246	PDE4DIP	4.01E-15	0.720788
247	ABCA1	3.26E-13	0.725883
248	VEGFC	4.17E-10	0.729634
249	KLF5	3.55E-14	0.729689
250	S100A4	3.09E-09	0.733081
251	FRMD6	5.85E-11	0.735752
252	BAMBI	1.92E-09	0.736896
253	CD9	7.39E-12	0.737787
254	TNNI2	9.86E-08	0.742044
255	EDEM2	9.01E-13	0.754455
256	PTHLH	9.27E-15	0.76346
257	ENPP1	1.94E-14	0.774618

Table 2 A total of 316 differentially expressed genes (DEGs) of GSE35614 identified by R statistical analysis. Cutoff criteria given as logFC < 0.5 and P.Value <0.05 (Cont.)

Sl.No.	Symbols.ch2	BH.corrected.pvalue	fold.change.mean
		Down-regulated DEGs	
258	SERPINB1	2.91E-11	0.776655
259	VCAN	8.92E-13	0.777873
260	LMO2	8.02E-14	0.778659
261	TOR3A	5.29E-13	0.779232
262	MMRN1	5.07E-11	0.783967
263	NDRG1	2.84E-14	0.784835
264	MEOX2	1.91E-05	0.792641
265	PCOLCE2	3.67E-10	0.793318
266	SLC4A4	1.57E-12	0.800968
267	CLIC2	2.22E-14	0.802212
268	MGST1	5.66E-13	0.807463
269	APLNR	1.19E-11	0.807896
270	ANGPT2	1.73E-14	0.810664
271	COL3A1	2.26E-12	0.814544
272	KRT8	2.50E-12	0.816987
273	ZNF521	5.12E-13	0.828886
274	IGFBP6	0.000537	0.829189
275	MT1A	2.05E-12	0.837721
276	COL15A1	6.08E-13	0.842404
277	ENPP2	2.17E-12	0.846881
278	ASPN	3.18E-12	0.85275
279	SAA3	2.66E-11	0.852779
280	MYOT	4.80E-12	0.861957
281	C10H15orf48	5.67E-05	0.875433
282	FBN1	1.53E-09	0.883592
283	MYH8	3.97E-14	0.896893
284	MYOZ2	2.05E-10	0.898751
285	SCARA5	8.55E-15	0.907877
286	CILP	7.80E-15	0.91024
287	SLN	2.22E-12	0.913423
288	ARSK	4.81E-14	0.916664
289	PDZK1IP1	7.23E-13	0.918921
290	LY6G5B	1.29E-11	0.946284
291	COL1A2	1.15E-07	0.958797
292	ADGRL4	1.11E-12	0.95995
293	BOLA-DQA5	9.98E-13	0.966275
294	NRP1	5.62E-13	0.972471
295	NUCB2	5.32E-10	0.982564
296	RARRES1	4.91E-12	0.993957
297	IGSF10	1.36E-11	0.994768
298	PROM2	1.83E-14	1.001274
299	ENPP5	2.06E-14	1.017065
300	C7	2.05E-13	1.019345

Table 2 A total of 316 differentially expressed genes (DEGs) of GSE35614 identified by R statistical analysis. Cutoff criteria given as logFC < 0.5 and P.Value <0.05 (Cont.)

Sl.No.	Symbols.ch2	BH.corrected.pvalue	fold.change.mean
Down-regulated DEGs			
301	TM4SF18	6.90E-14	1.025298
302	CCN3	1.53E-14	1.05023
303	EFEMP1	1.63E-09	1.053963
304	SPP1	1.00E-11	1.061779
305	FN1	2.33E-12	1.062287
306	ANXA1	4.05E-14	1.069078
307	KLHL41	2.16E-08	1.092996
308	MFAP5	6.86E-12	1.135965
309	TNNC2	0.001101	1.2055
310	MYL2	2.76E-13	1.206489
311	SERPINE2	7.34E-15	1.2375
312	TTN	1.11E-12	1.25311
313	MYL1	1.35E-09	1.302365
314	MATN2	2.39E-10	1.310824
315	MYH2	6.31E-15	1.489351
316	SERPINF1	1.03E-11	1.896521

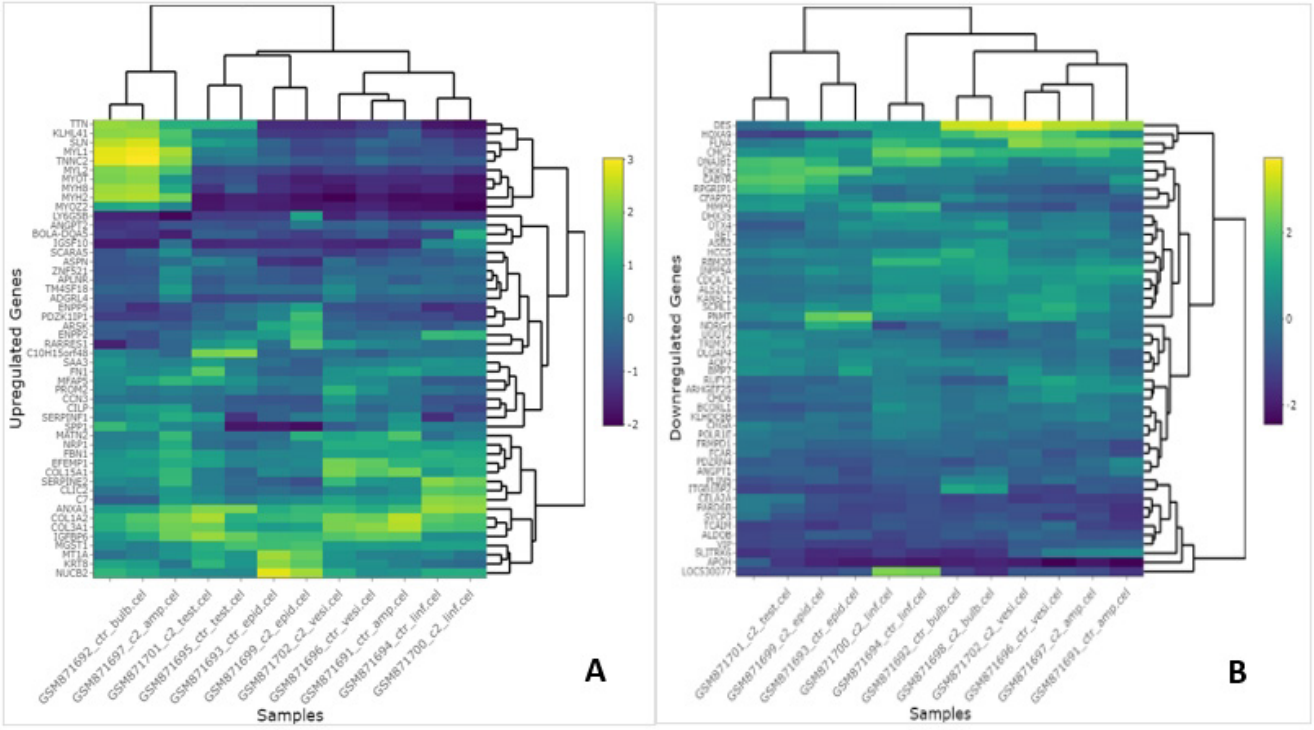

Figure 2 The heatmap shows the top 50 genes of (A) upregulated & (B) downregulated DEGs. Yellow colour indicates relatively high level of expression and blue colour indicates a relatively low level of expression. DEGs were identified by the criteria of |logFC| > 0.5 and P.value <0.05.

KEGG pathway enrichment and GO analysis of DEGs

All DEGs were uploaded to the DAVID online tool pathway enrichment analysis. For KEGG pathway enrichment (Figure 3A & Table 5), the DEGs mainly enriched in were ECM-receptor interaction, focal adhesion, cell adhesion molecules, arginine and proline metabolism, protein digestion and absorption. For the GO biological process analysis (Figure 3B & Table 3), the DEGs enriched in were angiogenesis, positive regulation of transcription-DNA-templated, cell adhesion, negative regulation of BMP signaling pathway, cell adhesion mediated by integrin, positive regulation of focal adhesion assembly, regulation of cell shape, cell differentiation, negative regulation of cell proliferation, endothelial cell migration.

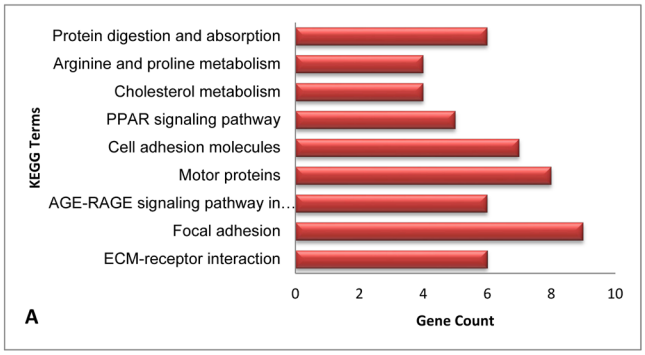

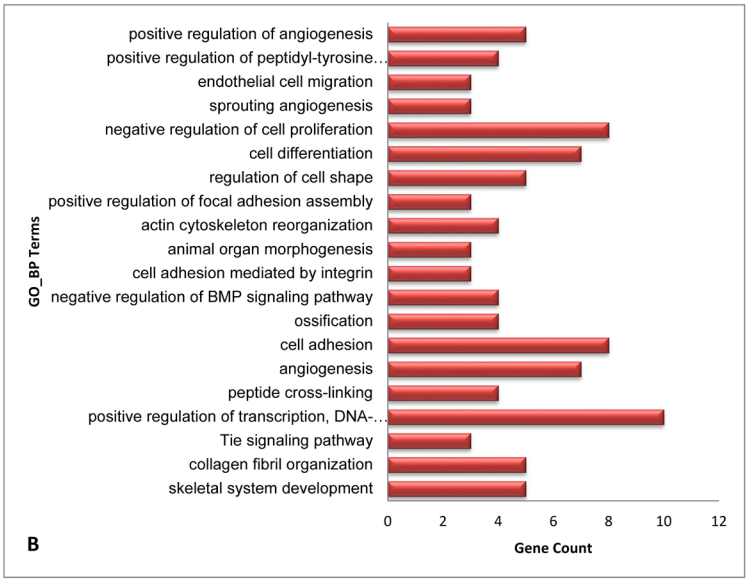

Figure 3 DAVID enrichment analysis. Enrichment analysis for (A) KEGG pathways and (B) GO terms of differentially expressed genes in sample of rams experimentally infected with a rough virulent strain of *Brucella ovis* (chronic 2 phase).

Table 3 Gene Ontology (GO) terms associated with differentially expressed genes (DEGs) along with its P.Value <0.05 and gene count >2

Sl.No	Term	Count	P.Value	Genes
1	skeletal system development	5	1.32E-03	COL1A2, COL5A2, MMP9, PTHLH, FBN1
2	collagen fibril organization	5	1.49E-03	COL3A1, TNXB, COL1A2, LUM, COL5A2
3	Tie signaling pathway	3	2.22E-03	ANGPT2, ANGPT1, TEK
4	positive regulation of transcription, DNA-templated	10	2.46E-03	RET, SMARCD3, MDFIC, NFIB, CDH1, TGFB3, BAMBI, TP53INP2, SPP1, TNNI2
5	peptide cross-linking	4	3.24E-03	COL3A1, ANXA1, FN1, TGM2
6	angiogenesis	7	0.003559	NRP1, EMCN, KLF5, ANGPT2, ANGPT1, EIF2AK3, CCN3
7	cell adhesion	8	0.006138	CLDN11, DPP4, SPON1, VCAN, TNFAIP6, SPP1, FN1, CD47
8	bone mineralization	4	0.012339	CLEC3B, COL1A2, ASPN, PTHLH
9	ossification	4	0.013424	MGP, SPP1, EIF2AK3, MMP9
10	negative regulation of BMP signaling pathway	4	0.016996	TNFAIP6, BAMBI, HTRA1, SOSTDC1
11	cell adhesion mediated by integrin	3	0.018478	MMRN1, CCN3, FBN1
12	animal organ morphogenesis	3	0.023888	NRP1, VEGFC, FLI1
13	actin cytoskeleton reorganization	4	0.028878	NRP1, ANXA1, FLNA, ASB2
14	positive regulation of focal adhesion assembly	3	0.029861	NRP1, TEK, S100A10
15	regulation of cell shape	5	0.030701	STRIP2, ANXA1, PALMD, BAMBI, FN1
16	cell differentiation	7	0.032431	SFRP4, PRM1, ANGPT2, ANGPT1, MGP, MYF6, TNP2
17	negative regulation of cell proliferation	8	0.03289	SFRP4, SCIN, SERPINE2, TGFB3, CDH13, CD9, NUPR2, NDRG1
18	sprouting angiogenesis	3	0.033047	ANGPT1, CDH13, TEK
19	endothelial cell migration	3	0.033047	DPP4, CDH13, FSTL1
20	positive regulation of peptidyl-tyrosine phosphorylation	4	0.044165	NRP1, ANGPT1, ENPP2, CD44
21	positive regulation of angiogenesis	5	0.04631	NRP1, PRKCB, VEGFC, TEK, CD34

Table 5 KEGG terms associated with differentially expressed genes (DEGs) along with its P.Value <0.05 and gene count >2

Sl.no	Term	Count	P.Value	Genes
1	ECM-receptor interaction	6	0.011128	TNXB, COL1A2, SPP1, FN1, CD47, CD44
2	Focal adhesion	9	0.011292	TNXB, COL1A2, PRKCB, MYL2, SPP1, FN1, FLNA, VEGFC, EMP1
3	AGE-RAGE signaling pathway in diabetic complications	6	0.017453	COL3A1, COL1A2, TGFB3, PRKCB, FN1, VEGFC
4	Motor proteins	8	0.026811	MYH1, MYH2, MYL1, MYL2, TNNT3, TNNC2, MYH8, TNNI2
5	Cell adhesion molecules	7	0.033237	CLDN11, VCAN, ALCAM, CDH1, SLITRK6, CLDN2, CD34
6	PPAR signaling pathway	5	0.033245	CPT1A, GK, ACOX1, AQP7, PLIN5
7	Cholesterol metabolism	4	0.040324	ABCA1, MYLIP, APOH, LIPA
8	Arginine and proline metabolism	4	0.046394	GATM, AOC1, MAOB, CKM
9	Protein digestion and absorption	6	0.046719	DPP4, COL15A1, COL3A1, COL1A2, COL5A2, COL21A1

PPI and module analysis of the DEGs

To explore the functional connection of all DEGs, PPI network was constructed using STRING database. A total of 316 DEGs were analyzed and then visualized by Cytoscape. As a result, there were 227 nodes and 515 edges in the PPI network, which represented proteins and functional protein-protein interactions (Figure 4A). Furthermore, functional modules were verified from PPI network by the MCODE plugin. The plugin detected 12 significant modules ranked by score were listed. Module 1 (score: 11.8) consisted of 12 nodes and 65 edges. Module 2 (score: 7) consisted of 8 nodes and 14 edges and module 3 (score: 4.2) consisted of 6 nodes and 8 edges. Most of the significant DEGs were gathered in the module 2.

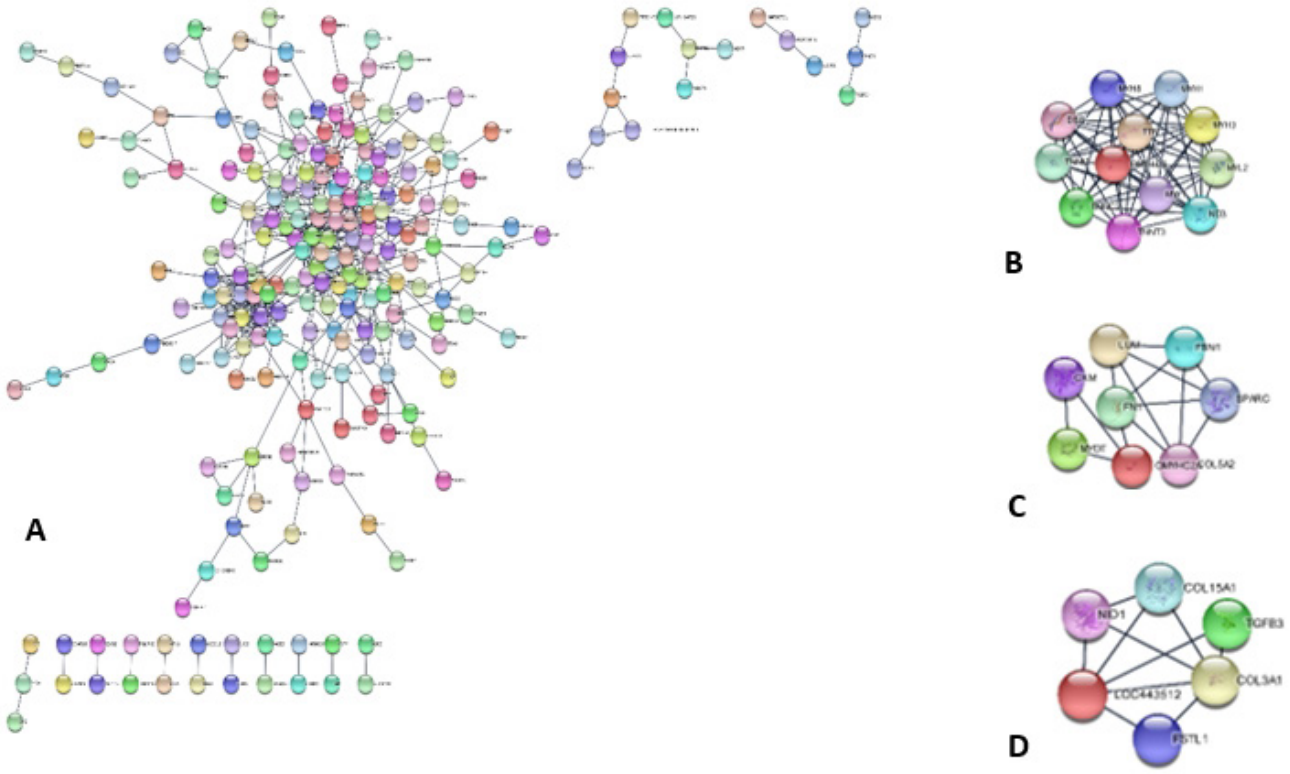

Figure 4 Protein-protein interaction network and module analysis of differentially expressed genes in GSE35614 dataset. (A) Protein-protein interaction network based on 227 DEGs constructed by Cytoscape. (A, B, C) Top three modules identified from the protein-protein interaction network.

Hub gene selection

To find the hub genes, the PPI network was downloaded as a simple interaction format (.tsv file), visualized with Cytoscape, and examined using the Cytohubba plugin. The top fifteen genes were obtained based on the three network parameters: degree, betweenness and closeness separately (Figure 5). Five genes, FN1 (Fibronectin I), FBN1 (Fibrillin 1), CDH1 (Cadherin 1), CD44 (Cluster of Differentiation 44), and SPP1 (Secreted Phosphoprotein 1), featured in all three lists were considered as hub genes.

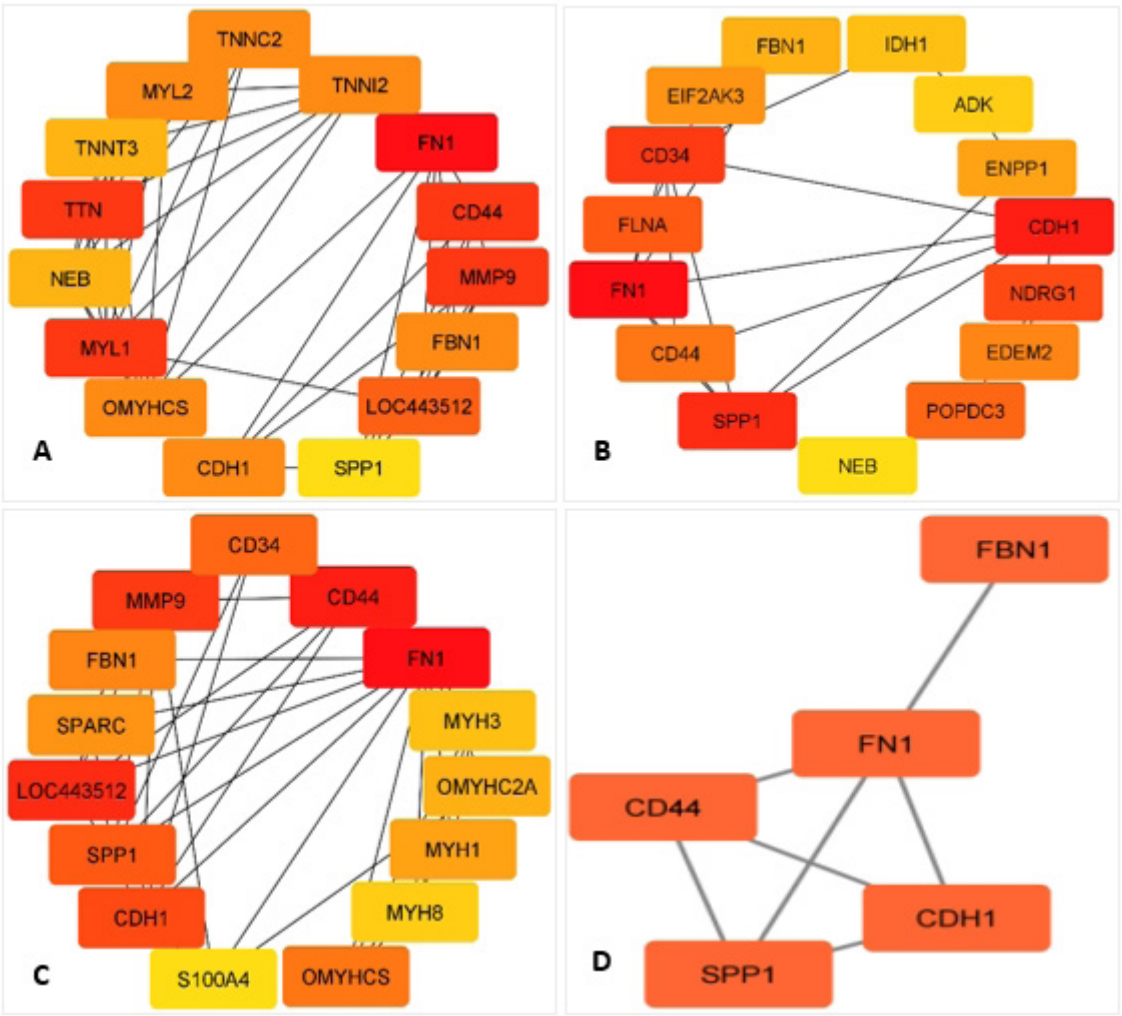

Figure 5 Hub genes identified using CytoHubba. Top 15 genes were identified based on (a) degree, (b) closeness and (c) betweenness parameters. (d) The common hub genes present in all three parameters.

DISCUSSION

Brucella ovis infection is one of the most important infectious cause that affects the reproduction in sheep globally. The rough virulent Brucella species, *B.ovis* causes clinical, subclinical, and chronic illness in sheep that is characterized by testicular changes leading to epididymitis, reduced fertility in rams, and sporadic miscarriages in ewes (Ficapal et al., 1998). The identification of this condition is challenging by testicular palpation alone due to the presence of additional bacteria producing symptomatic epididymitis (Blasco, 1990). Caprine studies on brucellosis in small ruminants were more common than ovine studies in terms of the quantity of animals used in the study. Additionally, there were very few molecular investigations on ovine brucellosis, a significant disease that primarily affects fertility and reproduction of sheep population. Brucellosis is endemic in India and is found across all regions, although its occurrence in sheep is considerably lower (7% in sheep in Sangrur district of Punjab) compared to other animal species in the country (Grewal, 2000). Understanding the gene regulation mechanisms and identifying key genes involved in Brucella ovis infection in India can inform regional knowledge gaps in epidemiology and serve as the foundation for developing targeted

treatment and prevention measures. This knowledge can lead to the creation of region-specific vaccines, diagnostics, and therapies, ultimately helping to mitigate the spread of the disease in the region and protect both livestock and public health.

Several microarray datasets of *Brucella ovis* in rams of different phases of infection were deposited in to NCBI GEO public data repository, such as GSE35614, GSE35613, and GSE35612. Since the *Brucella ovis* bacteria and its symptoms in sheep are largely expressed during the chronic phase of infection, the GSE35614 dataset was chosen in this study, which contains samples of rams infected with *Brucella ovis*. This data was then used to pinpoint the critical genes associated with the chronic phase of ovine brucellosis. Bioinformatics methods such as microarray differential gene expression analysis have proved helpful for making the most of the available gene expression data in the public domain. The majority of microarray experiments were conducted to examine gene expression patterns by examining the levels of hundreds of genes on a single platform (Wu et al., 2005). To further elucidate the function of the DEGs obtained from the differential analysis, functional annotation of the DAVID platform was used to conduct analysis of gene set enrichment and pathway analysis. The GO analysis annotates each DEG and enriches the DEGs that share the same attribute into a single term.

The main goal of this study was to identify the differentially expressed genes that were present in the dataset, regardless of the specific experimental setup used. Finding the genes that displayed appreciable changes in expression levels required comparing one or more pairs of samples. As a result, we extracted 316 DEGs, comprising 241 upregulated DEGs and 75 downregulated DEGs between the control and cases samples that had been exposed to *Brucella ovis* bacteria in a rough virulent strain. The DEGs enriched terms in the biological processes (BP) category were involved in angiogenesis, positive regulation of transcription- DNA-templated, cell adhesion mediated by integrin, negative regulation of BMP signaling pathway, cell adhesion, positive regulation of focal adhesion assembly, regulation of cell shape, cell differentiation, negative regulation of cell proliferation, endothelial cell migration (Figure 3A)**.** The genes involved in each functions are provided in Table 3. The key genes identified by cytoHubba plugin were also mainly enriched in the above functions. It is generally recognized that enhanced biological processes, such as angiogenesis and cell adhesion mediated by integrin, play a significant role in sheep reproduction. Spermatogenesis and gamete interactions require adhesion molecules like integrin, thus variations in integrin expression are connected to the release of spermatids into the tubule lumen (Preissner and Bronson, 2007). Integrins have also been found on germ cells, and it is well recognized that they are essential for the complicated physiological processes that lead to sperm-oocyte fusion (Merc et al., 2021). Sperms are unable to migrate through the UTJ (uterotubal junctions) when they are unable to bind to the integrins of the oviductal epithelium; however, the precise mechanism of this process is not yet established (Gabler et al., 2003). Numerous angiogenic and other factors, such as the vascular endothelial growth factor family, fibroblast growth factor, and angiopoietins (ANGPT), regulate the process of angiogenesis, which is the formation of new blood vessels from pre-existing vasculature. This process is crucial for the growth and development of all tissues, including the placenta (Reynolds and Redmer, 1995). The expression of several angiogenic factors

and their receptors in endometrial tissues during early pregnancy has been evaluated for several species including sheep (Reynolds et al., 2005). The placental life line connecting the maternal and foetal systems is thus vital for development, and when it is compromised, foetal growth and development are also impacted (Wulff et al., 2003; Burton et al., 2009). The BMP pathway is negatively or downregulated in cases of embryonic lethality. In vitro, BMP-4 stimulates endothelial cell migration, and when it is expressed erratically along the notochord, it causes the development of vascular plexuses (Nyamsuren et al., 2014). In severe infections linked to vascular leakage, the (Tie2) signalling pathway is noticeably unbalanced. The normal development of the embryonic vascular system requires functional Tie2 signalling (Parikh, 2017). Further research is also needed to understand how other enriched biological processes and pathways (such as collagen fibril organization, peptide cross-linkage, skeletal system development, motor protein, cholesterol metabolism, etc) in sheep is affected by *Brucella ovis* infection.

The uterine luminal epithelium is influenced by the Extracellular Matrix (ECM)-receptor pathway, one of the main pathways in which the DEGs are enriched. The discovery that significant alterations in the collagenous ECM, in which the theca and granulosa cells are embedded, are linked to both the growth and atresia of ovine ovarian follicles provides as an example of the importance of the ECM for follicular development (Huet et al., 1998; Berkholtz et al., 2006; Canty-Laird et al., 2010). The ECM-receptor interactions, focal adhesion, cell adhesion molecules, AGE-RAGE signaling pathway in diabetic complications, were the top relevant pathways (Figure 3A) with the highest reliability, as determined by the p-value. AGE/RAGE pathway plays a causal role in inflammation and specifically in diabetes-associated vascular complications (Jandeleit-Dahm et al., 2008). The Table 5 showed the exact DEGs implicated because there were numerous DEGs that were enriched in the different pathways. Most of the DEGs present in the Gene ontology and pathway analysis resulted in the upregulated genes. Therefore a separate analysis of downregulated genes had to be performed to identify the biological process of these genes. Thus the enrichment analysis of the downregulated DEGs resulted in biological process terms such as spermatogenesis, exchange of chromosomal proteins and nucleosome dissembly. Only three genes among 75 DEGs were involved in this process (Table 4), which indicate that the rest of the genes may not have met the required criteria after filtering. However the enriched terms spermatogenesis is highly related to epididymitis, a reproductive disorder in rams. Yarney et al.'s research (Yarney and Sanford, 1990) revealed a favourable correlation between testicular size and spermatogenic function. Ram lambs with larger testicles at six months of age produced more sperm daily and mated with ewes more frequently. The host's response to extravasated spermatozoa, rather than the virulence of *B. ovis*, is what causes the majority of the pathology that develops throughout the chronic illness phase. When the spermatozoa penetrate the tunica vaginalis cavity, granulomas form, which causes testicular atrophy (Foster, 2016). Thus when the upregulated DEGs gene groups are enriched in angiogenesis and cell adhesion, the downregulated genes inhibit the process of spermatogenesis and exchange of chromosomal protein.

Table 4 Gene ontology terms associated with down-regulated DEGs.

Sl. No	Term	Count	P.Value	Genes
1.	spermatogenesis, exchange of chromosomal proteins	2	0.018726	SYCP3, TNP1
2.	nucleosome disassembly	2	0.044366	SMARCD3, TNP1

Furthermore, we constructed the PPI network by all DEGs for the functional interaction (Figure 4A). The most significant three functional modules were filtered (Figure 4B, 4C, 4D). The modules identified represents highly interactive gene clusters among the PPI network of our DEGs. The hub genes constructed using the cytoHubba plugin of Cytoscape software revealed five hub genes (FN1, FBN1, CD44, CDH1, SPP1) among the top fifteen DEGs identified by the parameters such as degree, closeness and betweenness. Two of the hub genes FN1 and FBN1 were gathered in the module 2 with a high degree. FN1 (fibronectin 1) is an essential extracellular matrix glycoprotein in cell adhesion and migration (Dhanani et al., 2017). Collagen, fibrin, heparin, and integrins are among the ECM components that FN1 binds to in addition to cell surfaces (Akiyama et al., 1989). The study findings involving KEGG pathway enrichment analysis revealed that the ECM pathway may be connected to the symptoms of the disease, ovine brucellosis. In sheep, FN1 is involved in a number of activities involving cell adhesion and migration, including embryogenesis, wound healing, blood coagulation, host defense, cell shape maintenance, and opsonization (the process by which a pathogen is identified for phagocytosis) (Darribère and Schwarzbauer, 2000; Pulina et al., 2011; Dhanani et al., 2017). Increased ECM component deposition, especially FN, is recognized to be a contributing factor to the emergence of pathological states in fibrosis and inflammation-related disorders (Iwasaki et al., 2016; Dhanani et al., 2017). According to a study, superovulation during the mid-luteal phase, which corresponds to the beginning of embryonal identification in pregnant animals like sheep, had an impact on the expression of integrins as well as FN1. As a result, changing the expression (upregulation) of endometrial genes can affect the implantation of sheep via FN1, which is essential for embryo attachment and adhesion (Bedir et al., 2023). Osteopontin, also known as Secreted Phosphoprotein 1 (SPP1), is encoded by SPP1 gene. It was first shown to be a significant sialoprotein in the bone, assisting osteoclasts in binding to the calcified bone matrix. The SPP1 is necessary for critical biological functions including cancer, bone resorption, calcification, immune responses, wound healing, and developmental processes (Prince et al., 1987). It also performs ECM and intercellular communication functions (Yim et al., 2022). Upregulation of SPP1 gene expression is usually linked to inflammation brought on by conditions like infections, allergic reactions, autoimmune diseases, and tissue injury, among others. The gene was also found in the ovines' male and female reproductive systems. It also acts as a decapacitation factor that is expressed in the testes and epididymis. It interacts with integrins to alter fertilization by preventing early activation of the epididymal sperm's capacity to move or fertilize. Despite having various possible uses in the male reproductive system, SPP1 in rams' testicles plays a part in testicular cell adhesion during spermatogenesis and/or epididymal maturation. (Siiteri et al., 1995). Studies have shown that during the up-regulation, SPP1 in ovine is characterized by a complex temporal and spatial pattern of uterine and conceptus expression

involving immune, epithelial and, stromal cells (Garlow et al., 2002). As a result, changes in SPP1 expression can result in inflammatory illnesses such sheep brucellosis. Through integrin receptors, the hub gene CD44, a widely expressed cell surface marker and cell adhesion molecule, and the SPP1 genes control adhesion, migration, invasion, chemotaxis, and cell survival (Anborgh et al., 2010). Additionally, the association between the CD44 genes in sheep has only been the subject of relatively few investigations. $A\beta^{-/-}$ and C57BL/6 mice's $CD8^{+}$ T-lymphocytes exhibited a $CD44^{hi}$ $CD45RB^{lo}$ phenotype and a type 1 cytokine production profile with a lot of IFN-γ mRNA. Additionally, it was demonstrated that C57BL/6 CD8+ CTL may kill macrophages that are infected with Brucella (Oliveira and Splitter, 1995). Another hub gene was discovered, CDH1, which codes for the glycoprotein E-cadherin and is only expressed in epithelial tissues (Takeichi, 1995). It has been demonstrated that the cell-cell adhesion molecule CDH1 performs crucial roles in tissue architecture and embryogenesis by constructing intercellular junction complexes and establishing cell polarization (Frixen et al., 1991). CDH1 has been shown to execute important functions in embryogenesis and tissue architecture by forming intercellular junction complexes and establishing cell polarization in ovines (Van Roy and Berx, 2008). Additionally, a study discovered that CDH1 was expressed in sheep testis seminiferous tubules and undifferentiated spermatogonia through immunohistochemical analysis of frozen sections (Zhang Yan et al., 2014). The role of FBN1 hub gene was not yet identified in the context of sheep.

Although the clinical significance of FN1, SPP1, CDH1, and CD44 in *Brucella ovis* infection in sheep has not yet been established, we can infer from the above description that these genes were primarily involved in processes like angiogenesis, cell adhesions, and ECM complexes that seriously impair both male (rams) and female (ewes) sheep's reproductive health thus it can be potentially used as a clinical biomarker to identify the chronic pahse of ovine brucellosis. The relationship between germs and hosts is thought to begin with bacterial cell attachment, which is crucial for the emergence of disease. Because the field isolates have more or different forms of fimbrial and non-fimbrial adhesins or by the amount of their expression, relative to the reference strain, the over expression of genes involved in cell adhesion suggests the facilitation of entry of bacteria into the host cells (Bujold and MacInnes, 2015). The genes FN1, SPP1, and CDH1 were discovered to be more or less directly related to sheep and their biological reproductive pathways by influencing cell adhesion, embryogenesis, or fertilizing capacity in ewes and epididymal sperm in rams. Therefore, it was hypothesized that these three genes have significant effects on how the host reacts to *Brucella ovis* infection; however, further research is required to corroborate this hypothesis. The study also exposed the host reaction to *Brucella ovis* infection and pinpointed the essential genes that open new avenues for additional *in vivo* and *invitro* research into the causes and progression of ovine brucellosis.

Galindo et al.'s (Galindo et al., 2009) and Paula Antunes et al.'s (de Paula Antunes et al., 2015) earlier investigations used an *invitro* method to examine the gene expression of ovine infected with the virulent strain of *Brucella ovis* by taking samples directly from the host. Real-time qPCR analysis was performed after doing hybridization of the microarray data to acquire DEGs and to validate

the gene expression level. The result depicted that the pathogenicity of *B.ovis* in the infected tissue activates the immune response and the genes such as BOLA-DQA and BOLA-DQB were involved in the progression of infection in host. The JAK-STAT canonical pathway appears to be relevant during acute phase of infection and chronic phase I. Failure of JAK-STAT pathway can result in immune deficiency syndromes and cancer (Aaronson, 2002). In contrast, the 12 samples from GSE35614 were obtained 240 days after the challenge infection, and gene alterations in the rams during the chronic phase 2 were discovered using the analysis of these data. The varied levels of gene expression during ovine brucellosis are being examined for the first time using GSE35614. The current study has several advantages over earlier ones. First, this is a novel study that uses *insilico* bioinformatics to find DEGs. Second, specific hub genes connected to *Brucella ovis* infection in sheep were found by our investigation. The pathways and functions that were improved in the key DEGs were then further explored and demonstrated. Furthermore, we identified the hub genes or genes with high levels of connectivity, which show that they interact with or are linked to several other genes or proteins throughout the network. This in *silico* study offers prospective targets for the early detection and treatment of ovine brucellosis and sheds light on the molecular mechanism behind the alterations that take place in sheep during *Brucella ovis* infection.

CONCLUSIONS

Ovine brucellosis infected by *Brucella Ovis* bacteria cause serious reproductive illness in sheep. As a conclusion, our study discovered that the angiogenesis, cell adhesion mediated by integrin, spermatogenesis, and ECM interaction, were altered during *Brucella ovis* infection, thus further leading to reproductive health issues and causing brucellosis in ovines. These are found to be mediated by hub genes, based on the bioinformatics analysis of DEGs, GO keywords, KEGG pathway enrichment, and the PPI network. The current study offers a fresh approach for future research into the fundamental causes of sheep *Brucella ovis* infection onset and progression.

ACKNOWLEDGEMENTS

I would like to express my gratitude to the members of Spatial Epidemiology lab at the Indian Council for Agriculture Research (ICAR) — National Institute of Veterinary Epidemiology and Disease Informatics for their invaluable support in facilitating this research endeavor. I would also extend my appreciation to the HOD and esteemed professors from Bioinformatics Department of Sri Krishna Arts and Science College for their invaluable help and guidance.

AUTHOR CONTRIBUTIONS

VR designed, performed all the analysis and drafted the manuscript. UBI conceptualized the study. SR reviewed the paper. KPS, NNB and AP thoroughly analyzed and edited the manuscript. All the authors have read and approved the final manuscript.

REFERENCES

Aaronson, D.S., Horvath, C.M., 2002. A road map for those who don't know JAK-STAT. Science. 296(5573), 1653-1655.

Akiyama, S.K., Yamada, S.S., Chen, W.T., Yamada, K.M., 1989. Analysis of fibronectin receptor function with monoclonal antibodies: roles in cell adhesion, migration, matrix assembly, and cytoskeletal organization. J. Cell Biol. 109(2), 863-875.

Anborgh, P.H., Mutrie, J.C., Tuck, A.B., Chambers, A.F., 2010. Role of the metastasis-promoting protein osteopontin in the tumour microenvironment. J. Cell. Mol. Med. 14, 2037–2044.

Bashir, I., Rather, M.A., Rather, J.M., Hajam, I.A., Baba, J.A., Shah, M.M., Haq, Z.U., 2020. Study of mortality pattern in an organized farming sector amongst kashmir merino sheep. Int. J. Curr. Microbiol. Appl. Sci. 9, 1570–1578.

Bedir, Ö., Gram, A., Grazul-Bilska, A.T., Kowalewski, M.P., 2023. The effects of follicle stimulating hormone (FSH)-induced controlled ovarian hyperstimulation and nutrition on implantation-related gene expression in caruncular tissues of non-pregnant sheep. Theriogenology. 195, 229–237.

Berkholtz, C.B., Lai, B.E., Woodruff, T.K., Shea, L.D., 2006. Distribution of extracellular matrix proteins type I collagen, type IV collagen, fibronectin, and laminin in mouse folliculogenesis. Histochem. Cell. Biol. 126, 583–592.

Blasco, J.M., 1990. Brucella Ovis, In: Nielsen, K., Duncan, J.R. (Eds.), Animal Brucellosis, CRC Press, Florida, pp. 351–378.

Bujold, A.R., MacInnes, J.I., 2015. Identification of putative adhesins of Actinobacillus suis and their homologues in other members of the family Pasteurellaceae. BMC Res. Notes. 8, 1–13.

Burton, G.J., Charnock-Jones, D.S., Jauniaux, E., 2009. Regulation of vascular growth and function in the human placenta. Reproduction. 138, 895–902.

Canty-Laird, E., Carré, G.A., Mandon-Pépin, B., Kadler, K.E., Fabre, S., 2010. First evidence of bone morphogenetic protein 1 expression and activity in sheep ovarian follicles. Biol. Reprod. 83, 138–146.

Carrera-Chávez, J.M., Quezada-Casasola, A., Pérez-Eguia, E., Itzá-Ortíz, M.F., Gutiérrez-Hernández, J.L., Quintero-Elisea, J.A., Tórtora-Pérez, J.L., 2016. Sperm quality in naturally infected rams with Brucella ovis. Small Rumin. Res. 144, 220–224.

Darribère, T., Schwarzbauer, J.E., 2000. Fibronectin matrix composition and organization can regulate cell migration during amphibian development. Mech. Dev. 92, 239–250.

de Paula Antunes, J.M.A., Allendorf, S.D., Appolinário, C.M., Peres, M.G., Vicente, A.F., Cagnini, D.Q., de Castro Demoner, L., Figueiredo, P.R., Júnior, J.B., Galindo, R.C., 2015. Microarray analysis of gene expression in rams experimentally-infected with the virulent strain of brucella ovis. J Biotechnol Biomater. 5(4), 1000203.

Dhanani, K.C.H., Samson, W.J., Edkins, A.L., 2017. Fibronectin is a stress responsive gene regulated by HSF1 in response to geldanamycin. Sci. Rep. 7, 1–13.

Fang, X., Duan, S.F., Gong, Y.Z., Wang, F., Chen, X.L., 2020. Identification of key genes associated with changes in the host response to severe burn shock: a bioinformatics analysis with data from the Gene Expression Omnibus (GEO) database. J. Inflamm. Res. 13, 1029–1041.

Ficapal, A., Jordana, J., Blasco, J.M., Moriyón, I., 1998. Diagnosis and epidemiology of Brucella ovis infection in rams. Small. Rumin. Res. 29, 13–19.

Foster, R.A., 2016. Male genital system. In: Maxie, M.G. (Ed.) Jubb, kennedy & palmer's pathology of domestic animals: Volume 3, (6th edition). W.B. Saunders, Ontario, pp. 465-510.

Frixen, U.H., Behrens, J., Sachs, M., Eberle, G., Voss, B., Warda, A., Lochner, D., Birchmeier, W., 1991. E-cadherin-mediated cell-cell adhesion prevents invasiveness of human carcinoma cells. J. Cell. Biol. 113, 173–185.

Gabler, C., Chapman, D.A., Killian, G.J., 2003. Expression and presence of osteopontin and integrins in the bovine oviduct during the oestrous cycle. Reproduction. 126, 721–729.

Galindo, R.C., Muñoz, P.M., de Miguel, M.J., Marin, C.M., Blasco, J.M., Gortazar, C., Kocan, K.M., de la Fuente, J., 2009. Differential expression of inflammatory and immune response genes in rams experimentally infected with a rough virulent strain of Brucella ovis. Vet. Immunol. Immunopathol. 127, 295–303.

Garlow, J.E., Ka, H., Johnson, G.A., Burghardt, R.C., Jaeger, L.A., Bazer, F.W., 2002. Analysis of osteopontin at the maternal-placental interface in pigs. Biol. Reprod. 66, 718–725.

Grewal, S., Satinder, K., 2000. Survey of sheep and goat brucellosis in Sangrur district (Punjab, India). J. Parasitol. Appl. Anim. Biol. 9(2), 67-74.

Gupta, M.K., Behera, S.K., Dehury, B., Mahapatra, N., 2017. Identification and characterization of differentially expressed genes from human microglial cell samples infected with japanese encephalitis virus. J. Vector. Borne. Dis. 54, 131–138.

Hogue, C.W., Groll, M., 2001. An automated method for finding molecular complexes in large protein interaction networks. BMC. Bioinform. 29, 137–140.

Huet, C., Monget, P., Pisselet, C., Hennequet, C., Locatelli, A., Monniaux, D., 1998. Chronology of events accompanying follicular atresia in hypophysectomized ewes. Changes in levels of steroidogenic enzymes, connexin 43, insulin-like growth factor II/mannose 6 phosphate receptor, extracellular matrix components, and matrix metalloprotein. Biol. Reprod. 58, 175–185.

Iwasaki, A., Sakai, K., Moriya, K., Sasaki, T., Keene, D.R., Akhtar, R., Miyazono, T., Yasumura, S., Watanabe, M., Morishita, S., Sakai, T., 2016. Molecular mechanism responsible for fibronectin-controlled alterations in matrix stiffness in advanced chronic liver fibrogenesis. J. Biol. Chem. 291, 72–88.

Jandeleit-Dahm, K., Watson, A., Soro-Paavonen, A., 2008. The AGE/RAGE axis in diabetes-accelerated atherosclerosis. Clin. Exp. Pharmacol. Physiol. 35, 329–334.

Karimizadeh, E., Sharifi-zarchi, A., Nikaein, H., Salehi, S., Salamatian, B., Elmi, N., 2019. Analysis of gene expression profiles and protein-protein interaction networks in multiple tissues of systemic sclerosis. BMC. Med. Genom. 2, 1–12.

Liu, Y., Yi, Y., Wu, W., Wu, K., Zhang, W., 2019. Bioinformatics prediction and analysis of hub genes and pathways of three types of gynecological cancer. Oncol. Lett. 18, 617–628.

McFarlane, D., Salisbury, R.M., Osborne, H.G., Jebson, J.L., 1952. Investigation into sheep abortion in New Zealand during the 1950 lambing season. Aust. Vet. J. 28, 221–226.

Meltzer, E., Sidi, Y., Smolen, G., Banai, M., Bardenstein, S., Schwartz, E., 2010. Sexually transmitted brucellosis in humans. Clin. Infect. Dis. 51(2), e12-e15.

Menzies, P.I., 2012. Vaccination programs for reproductive disorders of small ruminants. Anim. Reprod. Sci. 130, 162–172.

Merc, V., Frolikova, M., Komrskova, K., 2021. Role of integrins in sperm activation and fertilization. Int. J. Mol. Sci. 22(21), 11809.

Oliveira, S.C., Splitter, G.A., 1995. CD8+ Type 1 CD44hi CD45 RBlo T lymphocytes control intracellular Brucella abortus infection as demonstrated in major histocompatibility complex class I- and class II-deficient mice. Eur. J. Immunol. 25, 2551–2557.

Pappas, G., Papadimitriou, P., Akritidis, N., Christou, L., Tsianos, E.V., 2006. The new global map of human brucellosis. Lancet. Infect. Dis. 6(2), 91–99.

Parikh, S.M., 2017. The angiopoietin-Tie2 signaling axis in systemic inflammation. J. Am. Soc. Nephrol. 28, 1973–1982.

Poester, F.P., Samartino, L.E., Santos, R.I., 2013. Pathogenesis and pathobiology of brucellosis in livestock. OIE. Rev. Sci. Tech. 32, 105–115.

Preissner, K.T., Bronson, R.A., 2007. The role of multifunctional adhesion molecules in spermatogenesis and sperm function: Lessons from hemostasis and defense? Semin. Thromb. Hemost. 33, 100–110.

Prince, C.W., Oosawa, T., Butler, W.T., Tomana, M., Bhown, A.S., Bhown, M., Schrohenloher, R.E., 1987. Isolation, characterization, and biosynthesis of a phosphorylated glycoprotein from rat bone. J. Biol. Chem. 262, 2900–2907.

Pulina, M.V., Hou, S.Y., Mittal, A., Julich, D., Whittaker, C.A., Holley, S.A., Hynes, R.O., Astrof, S., 2011. Essential roles of fibronectin in the development of the left-right embryonic body plan. Dev. Biol. 354, 208–220.

Rajashekara, G., Eskra, L., Mathison, A., Petersen, E., Yu, Q., Harms, J., And, Splitter, G., 2006. Brucella: functional genomics and host–pathogen interactions. Anim. Health Res. Rev. 7(1-2), 1-11.

Reynolds, L.P., Borowicz, P.P., Vonnahme, K.A., Johnson, M.L., Grazul-Bilska, A.T., Redmer, D.A., Caton, J.S., 2005. Placental angiogenesis in sheep models of compromised pregnancy. J. Physiol. 565, 43–58.

Reynolds, L.P., Redmer, D.A., 1995. Utero-placental vascular development and placental function. J. Anim. Sci. 73, 1839–1851.

Seleem, M.N., Boyle, S.M., Sriranganathan, N., 2010. Brucellosis: a re-emerging zoonosis. Vet. Microbiol. 140, 392–398.

Shome, R., Sahay, S., Triveni, K., Krithiga, N., Shome, B.R., Rahman, H., 2018. Evidence of ovine brucellosis due to Brucella ovis and Brucella melitensis in Karnataka, India. Indian. J. Anim. Sci. 88, 522–525.

Siiteri, J.E., Ensrud, K.M., Moore, A., Hamilton, D.W., 1995. Identification of osteopontin (OPN) mRNA and protein in the rat testis and epididymis, and on sperm. Mol. Reprod. Dev. 40, 16–28.

Takeichi, M., 1995. Morphogenetic roles of classic cadherins. Curr. Opin. Cell Biol. 7, 619–627.

Van Roy, F., Berx, G., 2008. The cell-cell adhesion molecule E-cadherin. Cell. Mol. Life Sci. 65, 3756–3788.

Watt, D.A., 1970. T esticular Abnormalities and Spermatogenesis in the Merino Ram (Master's Thesis). University of Sydney.

Wu, W., Dave, N., Tseng, G.C., Richards, T., Xing, E.P., Kaminski, N., 2005. Comparison of normalization methods for CodeLink Bioarray data. BMC. Bioinform. 6, 1–14.

Wulff, C., Weigand, M., Kreienberg, R., Fraser, H.M., 2003. Angiogenesis during primate placentation in health and disease. Reproduction. 126, 569–577.

Yarney, T.A., Sanford, L.M., 1990. Pubertal development of ram lambs: reproductive hormone concentrations as indices of postpubertal reproductive function. Can. J. Anim. Sci. 70, 149–157.

Yim, A., Smith, C., Brown, A.M., 2022. Osteopontin/secreted phosphoprotein-1 harnesses glial-, immune-, and neuronal cell ligand-receptor interactions to sense and regulate acute and chronic neuroinflammation. Immunol. Rev. 311(1), 224-233.

Zhang, Y., Wu, S., Luo, F.H., Baiyinbatu, Liu, L.H., Hu, T.Y., Yu, B., Li, G.P., Wu, Y.J., 2014. CDH1, a novel surface marker of Spermatogonial stem cells in sheep testis. J. Integr. Agric. 13(8), 1759-1765.

Zhu, W., Nan, Y., Wang, S., Liu, W., 2019. Bioinformatics analysis of gene expression profiles of sex differences in ischemic stroke. Biomed. Res. Int, 2019, 2478453.

How to cite this article;

Varsha Ramesh, Uma Bharathi Indrabalan, Swati Rani, Kuralayanapalya Puttahonnappa Suresh, Nagendra Nath Barman and Azhahianambi Palavesam. Unravelling key genes associated with ovine Brucellosis by differential gene expression analysis: A holistic bioinformatics study. Veterinary Integrative Sciences. 2024; 22(1): 419 - 444